Multi-Temporal Mapping of Built-up Areas Using Daytime and Nighttime Satellite Images Based on Google Earth Engine Platform

S. Hutasavi, D. Chen

***Abstract*—**The built-up area is a significant proxy to measure regional economic growth and reflects the Gross Provincial Product (GPP). However, an up-to-date and reliable database of built-up areas is not always available, especially in developing countries. The cloud-based geospatial analysis platform such as Google Earth Engine (GEE) provides an opportunity with accessibility and computational power for those countries to generate the built-up data. Therefore, this study aims to extract the built-up areas in Eastern Economic Corridor (EEC), Thailand using day and nighttime satellite imagery based on GEE facilities. The normalized indices were generated from Landsat 8 surface reflectance dataset, including Normalized Difference Built-up Index (NDBI), Built-up Index (BUI), and Modified Built-up Index (MBUI). These indices were applied to identify built-up areas in EEC. The result shows that MBUI performs better than BUI and NDBI, with the highest accuracy of 0.85 and Kappa of 0.82. Moreover, the overall accuracy of classification was improved from 79% to 90%, and error of total built-up area was decreased from 29% to 0.7%, after night-time light data from the Visible and Infrared Imaging Suite (VIIRS) Day Night Band (DNB). The results suggest that MBUI with night-time light imagery is appropriate for built-up area extraction and be utilize for further study of socioeconomic impacts of regional development policy over the EEC region.

***Keywords*—**Built-up area extraction, Google earth engine, adaptive thresholding method, rapid mapping.

I. Introduction

RECENTLY, the geospatial data have been used as significant proxy indicators for quantifying, measuring, and illustrating the human activities such as economic growth in the vicinity [1]. For instance, [2] found that the built-up area is highly correlated with various socioeconomic data such as real Gross Domestic Product (GDP), total population and employment, indicating a strong relationship between built-up areas and the industry development in seven main cities across Canada.

EEC area covers three rural provinces (Rayong, Chonburi, and Chachoengsao) in Thailand. The EEC development policy aims to improve economic development and enhance the people's quality of life and well-being. Therefore, built-up areas have been rapidly changed through intensively implementing industrial development policies in the last two decades. However, the availability of annually built-up areas dataset in developing country such as Thailand is still limited.

Remotely sensed data from satellites provide an alternative way to extract build-up areas. Among those satellite images, Landsat imagery is one with the longest history. Many previous studies have identified built-up areas extracted from Landsat multispectral image using the spectral indices such as NDBI, BUI, MBUI, Urban Index (UI), Index-based Built-up Index (IBI), Enhanced Built-up and Bareness Index (EBBI) [2]-[7]. Also, the nighttime satellite images are widely adopted for urban extraction, for example, [9] highlighted the usefulness of Landsat and nighttime light fusion dataset to classify built-up land cover [8]. Moreover, Duque et al. analyzed the urban growth dynamic from 1996 to 2010 using nighttime light imageries to reveal the urban expansion and urban growth form [9].

This study aims to identify the most suitable index and the effect of incorporating nighttime satellite images for built-up area extraction. The chosen indices include NDBI, BUI, and MBUI derived from Landsat 8 Surface Reflectance (LS8 SR) images. These indices had been adopted to identify built-up or urban area in Thailand, for example [3] developed MBUI index to extract built-up area in Samuthprakan province, Thailand. The result illustrated that MBUI performed best enhancement of the built-up area.

Nowadays, cloud-based computing platforms such as the GEE became more effective and constructive tools with a variety of satellite images and geospatial datasets [10], [11]. GEE allows users to conduct geospatial data analysis by providing various computation, analyzation, and visualization of geospatial datasets through the platform (https://earthengine.google.com). For example, Goldblatt et al. used GEE facilities to detect the urban area boundaries in India by applying three classifiers on Landsat 7 and 8 images [12]. GEE demonstrated the high potential in large-scale temporal urbanization analysis process. In 2020, Pu et al. utilized Landsat time series and computation algorithms in GEE to map urban areas and achieved an accuracy of 0.8 to 0.9 [11].

In this study, the processes based on GEE platform include (1) computing built-up indices from multi-temporal Landsat 8 surface reflectance datasets, (2) extracting light intensity and area of lit from VIIRS DNB, and (3) classifying the built-up areas from LS 8 SR, and LS 8 SR together with NTL using adaptive thresholding method (Otsu's threshold) (see Fig. 1). Then, the extraction accuracy was assessed and compared based on 500 sampling random points from the national land use

S. Hutasavi is Ph.D. candidate of Dept. of Geography and Planning, Queen's University, Kingston, Ontario, K7L 3N6, Canada (phone: 343-363-6518; e-mail: 16sh48@queensu.ca).

dataset and virtual ground truth from LS 8 SR images.

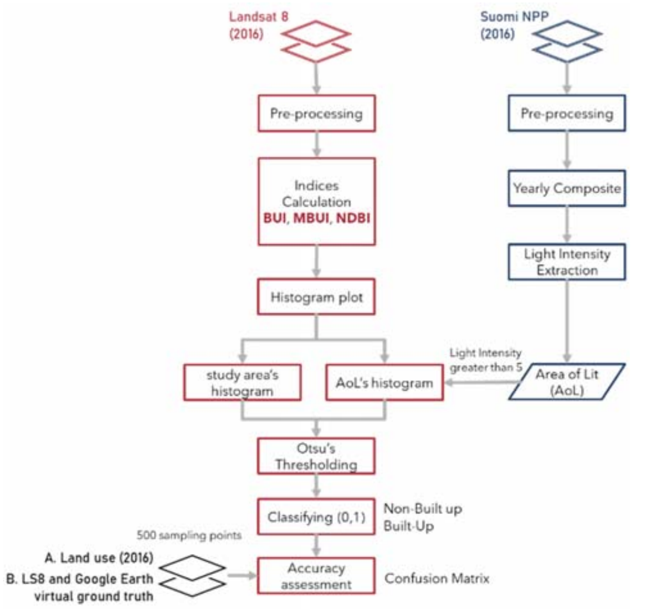

Fig. 1 Research study flow chart

II. Data and Methodology

A. Day-Time Satellite Imagery

Landsat 8 Surface reflectance (LS8 SR) dataset in GEE platform provided by USGS is the atmospherically corrected surface reflectance from the Landsat 8 OLI/TIRS sensors. The LS8 SR collection can be filtered by day, month, year, percent cloud coverage, and specific study area to select the appropriate images for a study. Here, cloud masking based on Landsat quality band was applied on all available images over the study area during 2016 to remove pixels which contain cloud and cloud shadows. Median composite was applied on the masked images to generate an annual composite.

B. Night-Time Satellite Imagery

The monthly average radiance composite images were derived from the VIIRS DNB on board of the Joint Polar-orbiting Satellite System Satellites (JPSS). We processed yearly average composite images and light intensity extraction using GEE platform.

C. Land Use Data

The 2016 land-use dataset from Geoinformatics and Space Development Agency (GISTDA), Thailand has been used as reference data. It was updated by virtual interpretation and ground survey method from the 2011 land-use dataset using THEOS (2 meters panchromatic and 15 meters multispectral resolution) and Landsat 8 images. The misclassification rate is ≤ 25% at kappa coefficient ≥ 75% and Root Mean Square Error (RMSEH) ≤ 14.4.

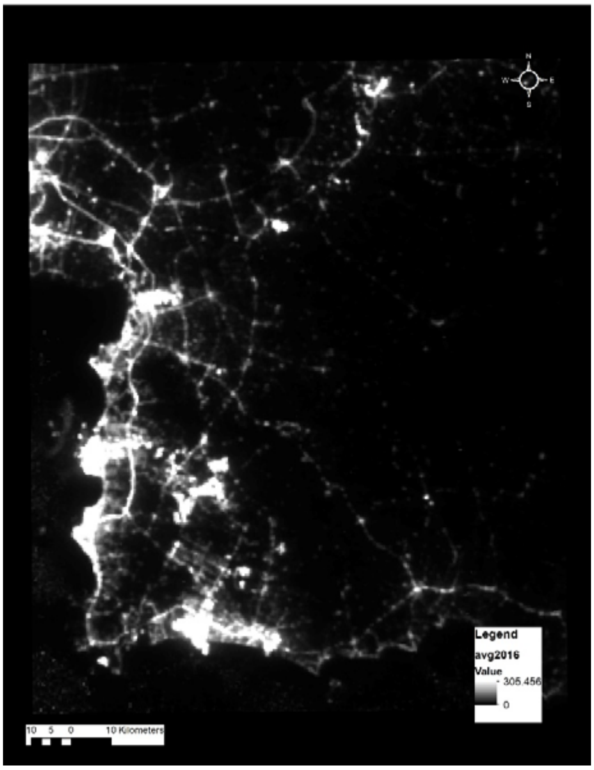

Fig. 2 (a) Nighttime Light from VIIRS DNB sensor

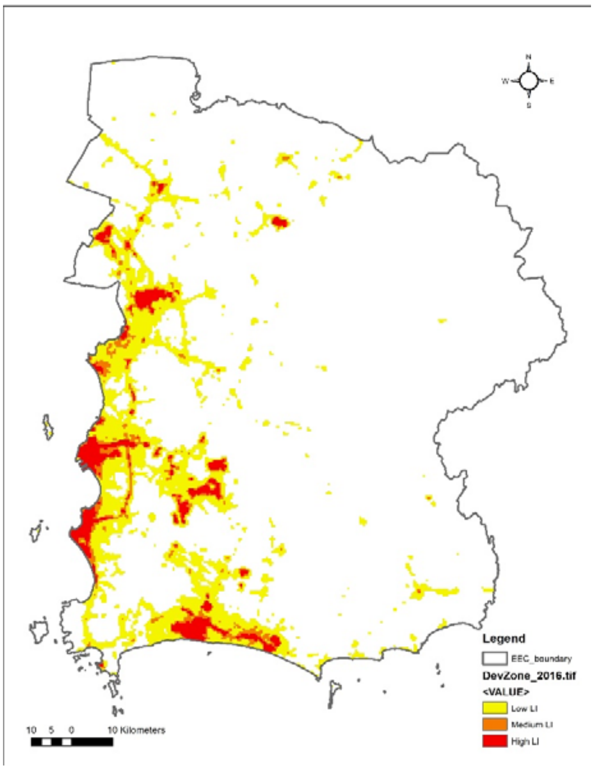

Fig. 2 (b) The area of lit was extracted from VIIRS DNB (created by the author via GEE platform)

D. Built-Up Area Indices

The general built-up indices including NDBI, BUI, and MBUI have been adopted in this study. Based on NIR and

SWIR spectrum, the NDBI was originally developed for Landsat TM with the multispectral sensor at SWIR band between 1.55-1.75 µm and a NIR band between 0.76-0.9 µm. The values of NDBI range from -1 to +1, the high value represents the built-up areas. The NDBI can be calculated by (1):

$$NDBI = \frac{(SWIR - NIR)}{(SWIR + NIR)} \quad (1)$$

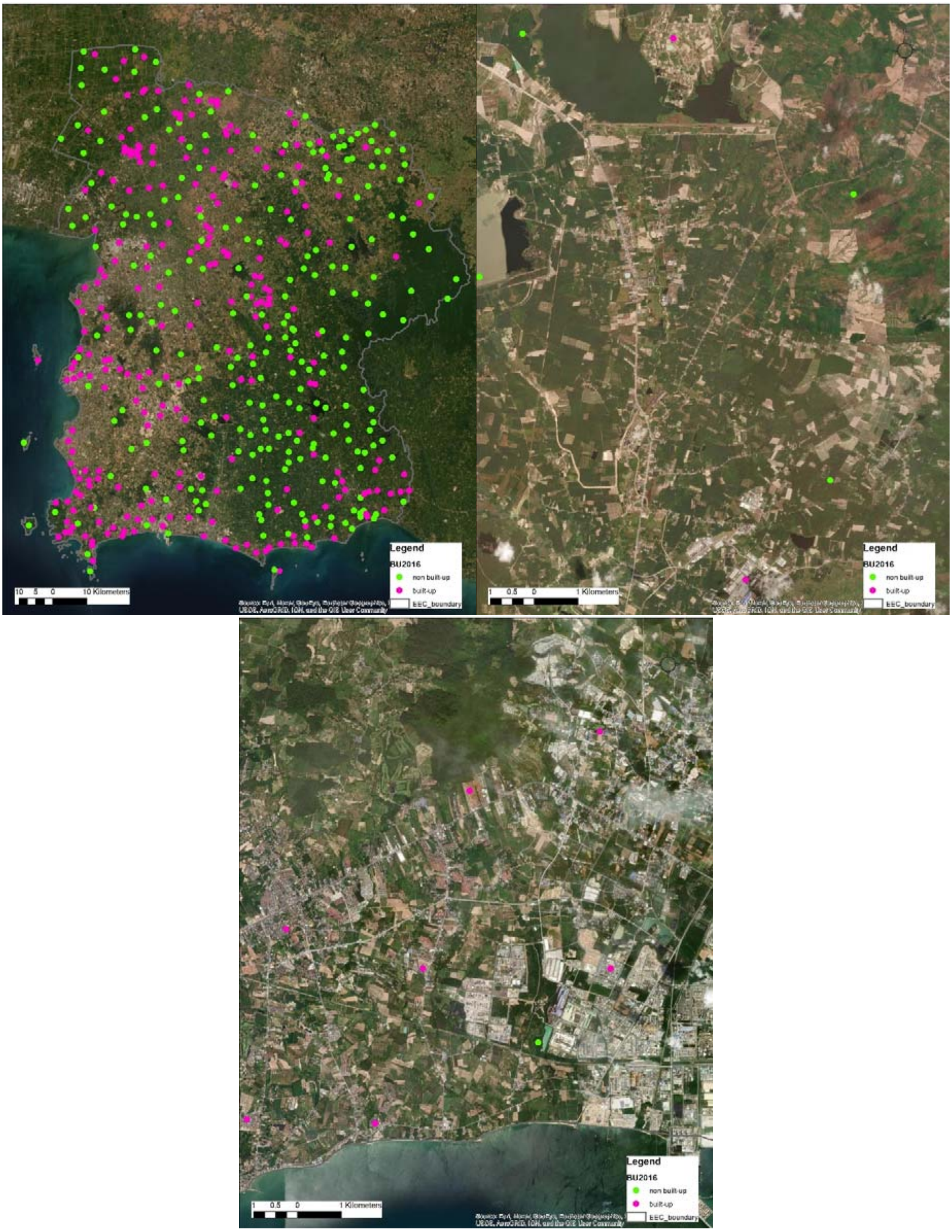

Fig. 3 Random sampling points used as reference data in the accuracy assessment. Red dots are built-up and green dots are non-built-up

BUI is based NDBI and NDVI. The computational result is a binary image where higher positive value is identified as built-up and bare area. The BUI can be calculated by (2):

$$BUI = NDBI - NDVI \quad (2)$$

MBUI is developed as an index aiming to enhance the quality of built-up areas classification technique [2]. It is an integration between BUI and Modified NDWI (MNDWI) to highlight the contrast between built-up and water areas and distinguish built-up and agriculture areas more precisely. The negative values of MBUI represent built-up areas while the positive value is water. The MNDWI and MBUI can be calculated by (3) and (4) respectively:

$$MNDWI = \frac{(Green - SWIR)}{(Green + SWIR)} \quad (3)$$

$$MBUI = BUI - MNDWI \quad (4)$$

The histogram of each index (NDBI, BUI, and MBUI) was calculated for both the whole study area and the area of lit extract from NTL dataset.

E. Extracting Build-Up Areas with Thresholding

To identify build-up areas from these index images, the simplest way is to apply thresholding which creates a binary image of build-up and non-build-up areas. Otsu's thresholding method is the effectual method that determines an optimal threshold value from an image histogram [13]. The Otsu's algorithm can be calculated by generating histogram of the difference image, then the pixel count at each bin i (gray level) is normalized as (5):

$$p_i = \frac{n_i}{N}, \text{i=1, 2, …, L} \quad (5)$$

where n_i is pixel number of bin i in the histogram; N is the total number of pixels; L is the total number of bins (grey levels) in the histogram.

The threshold was determined using the between-class variance $\sigma_B^2(t)$ at threshold t as calculated by:

$$\sigma_B^2(t) = \frac{[\mu_L P_t - \mu(t)]}{P_t[1 - P_t]} \quad (6)$$

where $P_t = \sum_{i=1}^{t} p_i$, $\mu_L = \sum_{i=1}^{L} ip_i$ and $\mu(t) = \sum_{i=1}^{t} ip_i$

The optimum threshold is given when the between-class variance $\sigma_B^2(t)$ is maximized [13]. To evaluate the impact from incorporating VIIRS data, the optimum thresholds were calculated and applied based on the histograms of the whole study area and the area of lit only.

F. Accuracy Assessment

500 random sampling points were generated over the study area and labeled as built-up and no-built up based on land use dataset and visual interpretation from LS8 (Fig. 3). The accuracy of built-up area extraction using Otsu's algorithm was compared between the extraction result from thresholding value that is calculated from (1) the histogram of NDBI, BUI, and MBUI in whole study area and (2) the histogram of NDBI, BUI, and MBUI in the area of lit.

III. Results and Discussion

A. Indice Results

The maps of the three indices are shown in Fig. 4. The histogram of each index for the whole study region, and only in the area of lit were illustrated in Figs. 5 (a) and (b). The BUI's histogram of the whole study area has two peaks (bimodal), while NDBI and MBUI have a plateau form. However, the histogram of each index from only the area of lit presents a more uniform distribution (Fig. 5 (b)). This different pattern observed resulted from the removal of influences from spectral characteristics under different land covers creating more uniform pattern.

The statistical summary of indices' histograms (Figs. 5 (a) and (b)) is reported in Table I along with the Otsu's threshold values calculated based on histograms of whole study area and the area of lit (AoL) only. The optimal thresholds for the whole study area are about 50% higher than that of the corresponding AoL.

TABLE I
HISTOGRAM STATISTIC SUMMARY OF INDICES

	LS8 (Pixel count = 56,120)			LS8+AoL (Pixel count = 8,716)		
	BUI	MBUI	NDBI	BUI	MBUI	NDBI
Mean	-0.795	-0.617	-0.187	-0.526	-0.331	-0.087
Standard Deviation	0.233	0.252	0.095	0.185	0.203	0.073
Variance	0.054	0.063	0.009	0.343	0.041	0.005
Thresholding Value	-0.795	-0.620	-0.191	-0.526	-0.345	-0.099

B. Comparison of Built-Up Areas Extraction between NDBI, BUI, MBUI, and These Indices with Incorporation of AoL

The thresholding values computed by Otsu's algorithm in Table I were used to classify built-up areas. The built-up areas based on the thresholding from the histogram of the whole study area are larger than both the one from that of AoL and the built-up areas from land use 2016 dataset (Fig. 6).

The performance of built-up area extraction is good with the overall accuracy of all indices over 0.80 (Table II), and precision over 0.7. MBUI shows better performance than BUI and NDBI, with the highest accuracy of 0.85 and Kappa of 0.81. Moreover, when night-time light data from VIIRS DNB were incorporated into the extraction process the precision of classification was improved from 79% to 90%, and the error of total built-up area was decreased from 29% to 0.7%.

LS 8

NDBI

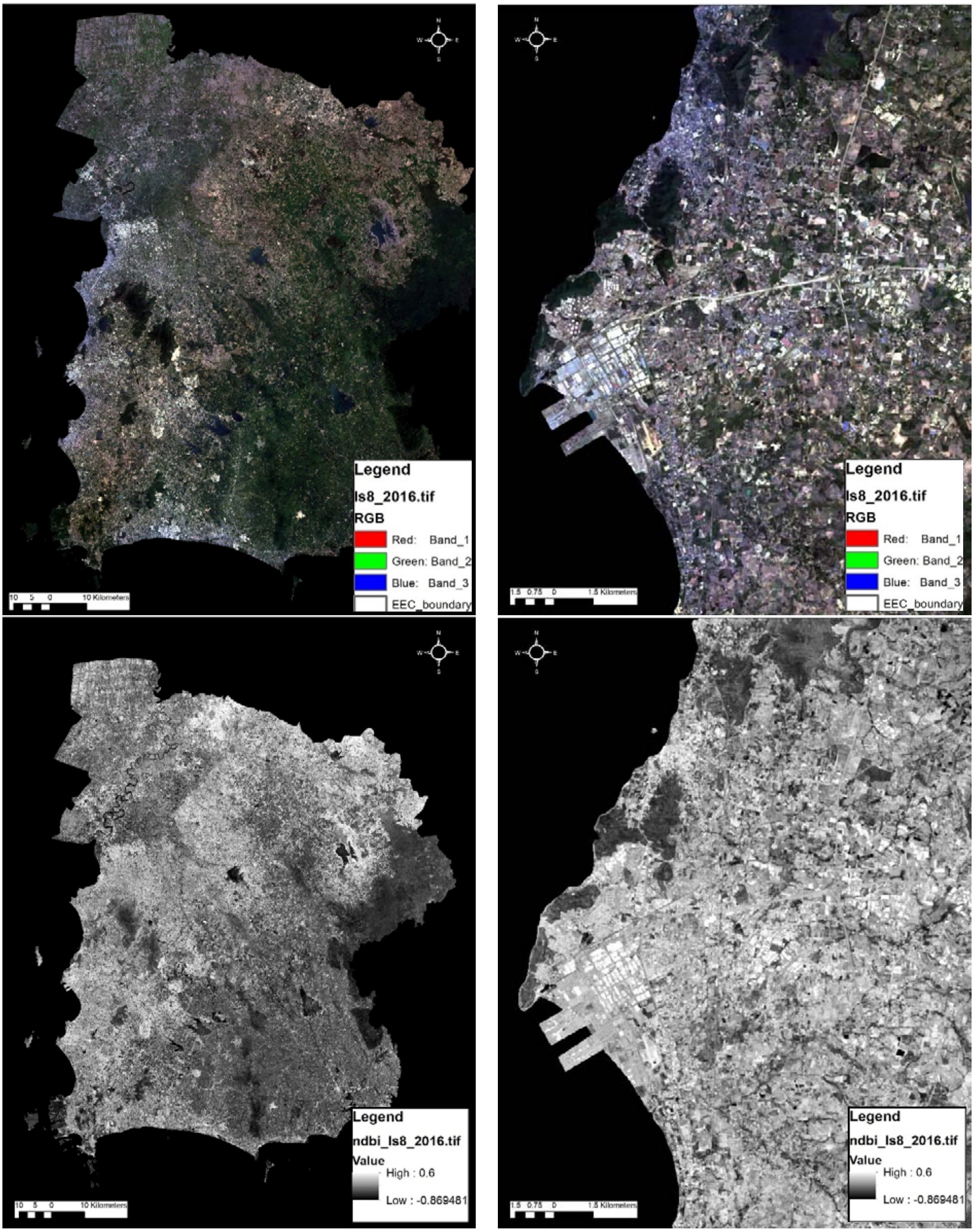
Legend
ls8_2016.tif
RGB
Red: Band_1
Green: Band_2
Blue: Band_3
EEC_boundary
10 5 0 10 Kilometers
1.5 0.75 0 1.5 Kilometers
Legend
ndbi_ls8_2016.tif
Value
High : 0.6
Low : -0.869481

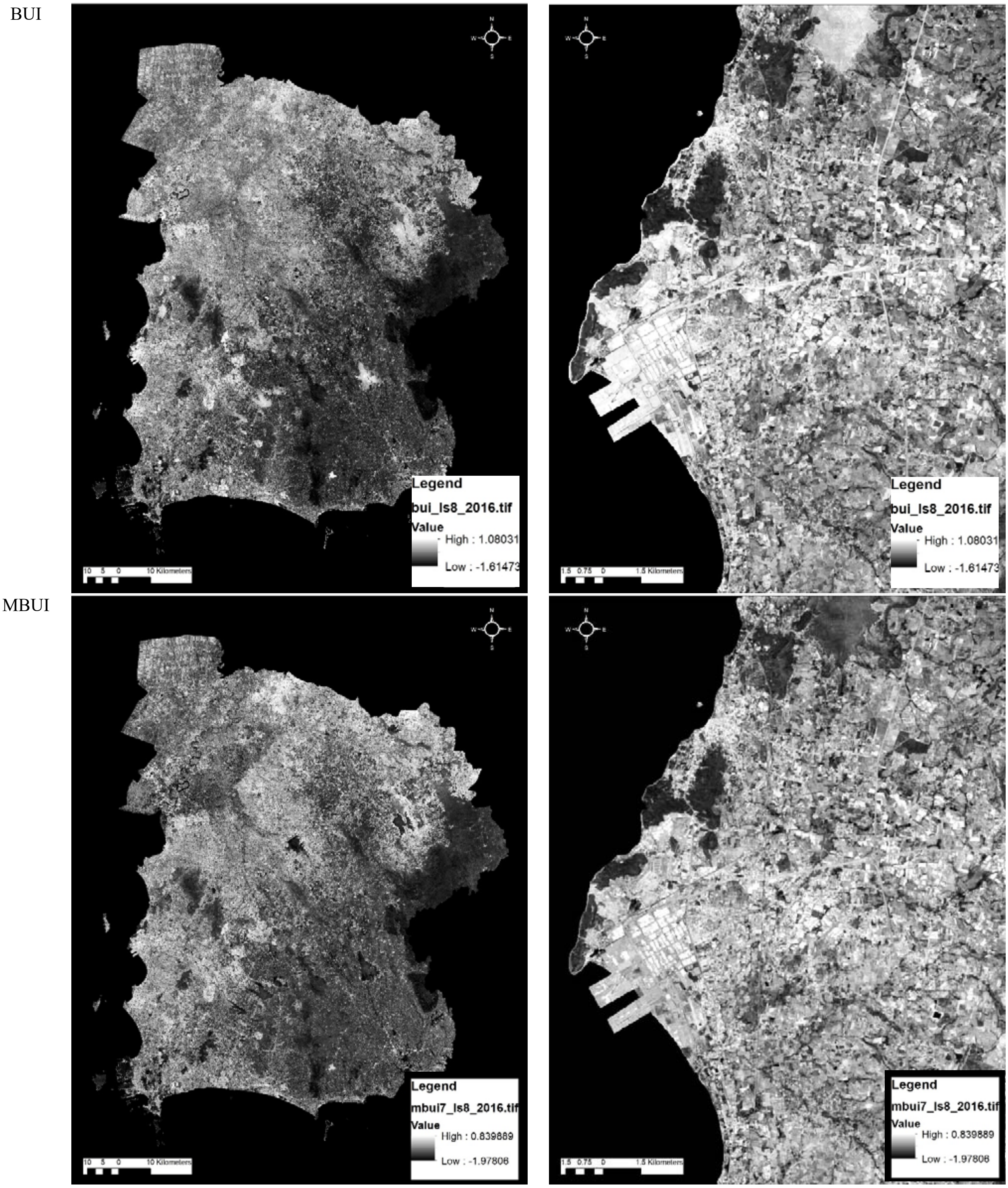

Fig. 4 Indices' computation results

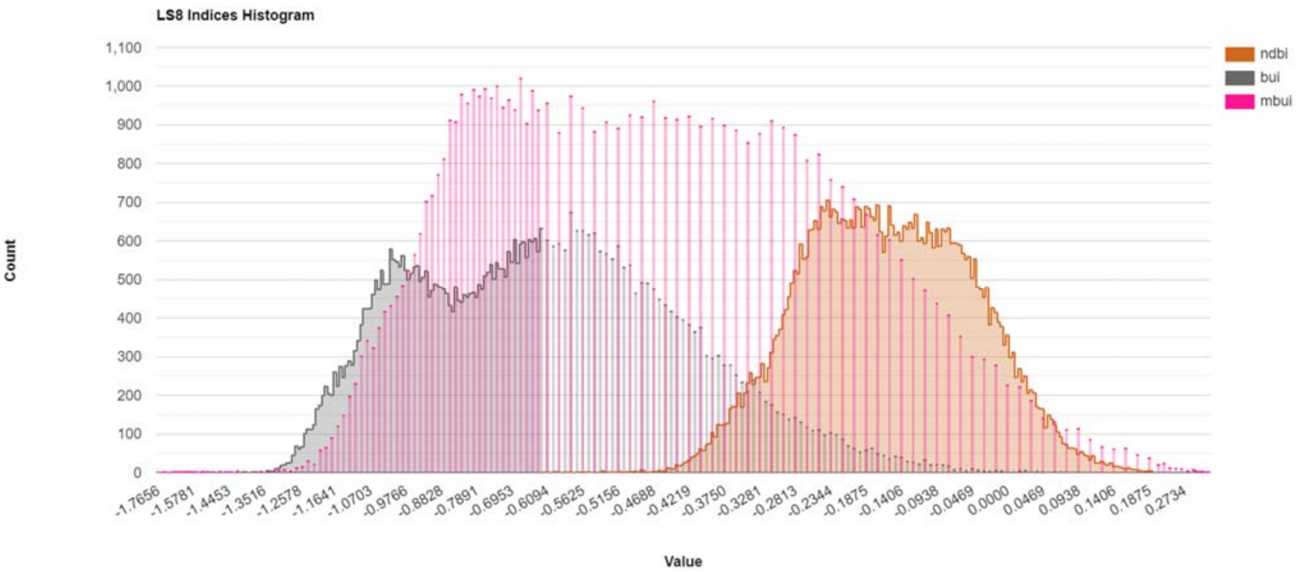

Fig. 5 (a) Histogram of indices for all pixels in whole study area

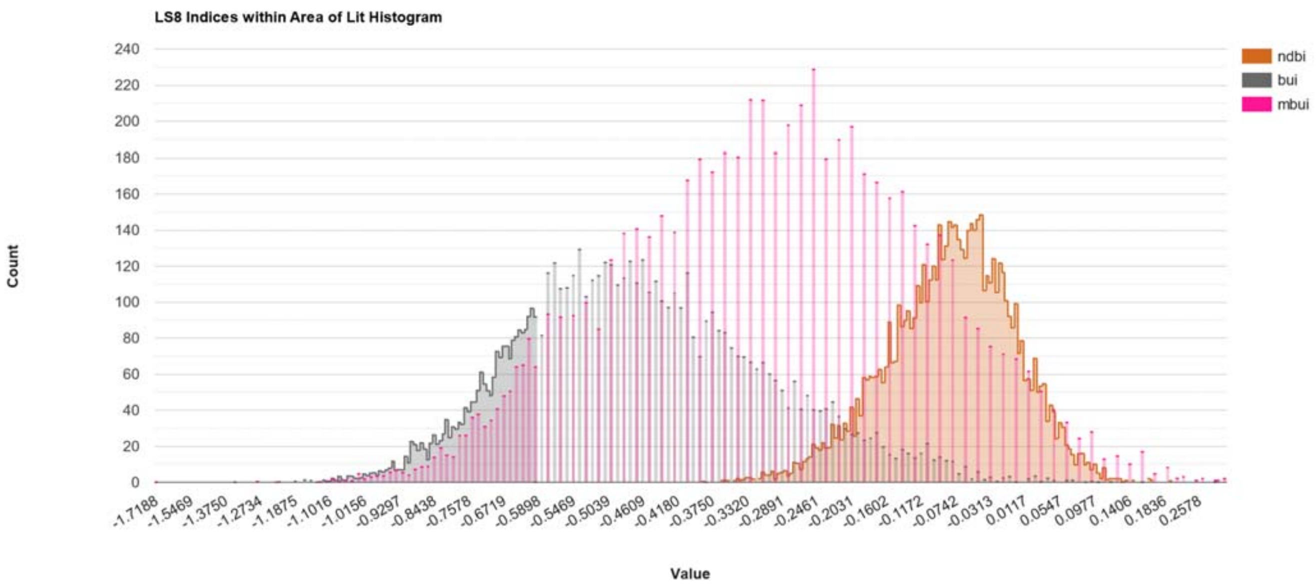

Fig. 5 (b) Histogram of indices for pixels in the area of lit

TABLE II
THE ACCURACY ASSESSMENT OF BUILT-UP AREAS CLASSIFICATION BY INDICES

	NTL	LS8			LS8+AoL		
	AoL	BUI	MBUI	NDBI	BUI	MBUI	NDBI
Accuracy	0.75	0.80	0.85	0.84	0.80	0.85	0.83
Misclassification rate	0.26	0.20	0.15	0.16	0.20	0.15	0.17
Precision	0.78	0.73	**0.79**	0.78	0.85	**0.90**	0.86
Kappa	0.74	0.75	0.81	0.80	0.75	0.82	0.79
Total built-up areas different (%)	13.01	34.72	**28.92**	33.28	1.76	**0.72**	5.81

IV. CONCLUSION

This study presents the evaluation of suitable optical indices and the incorporation of nighttime satellite imagery for built-up area extraction in Thailand EEC via GEE. The built-up area extraction results based on optimal Otsu's threshold values perform well, in terms of the overall accuracy and precision of the classification. The MBUI performed better than NDBI and BUI by reducing the misclassification of shallow water problems of BUI with MNDWI instead of NDWI in the formula. Furthermore, the AoL from nighttime light data helps improve the extraction accuracy, and significantly reduces the error of total built-up area in the study area. The prototype used in this study provides a rapid yearly built-up extraction method for further studying of socioeconomic impacts of regional development policy over the EEC region.

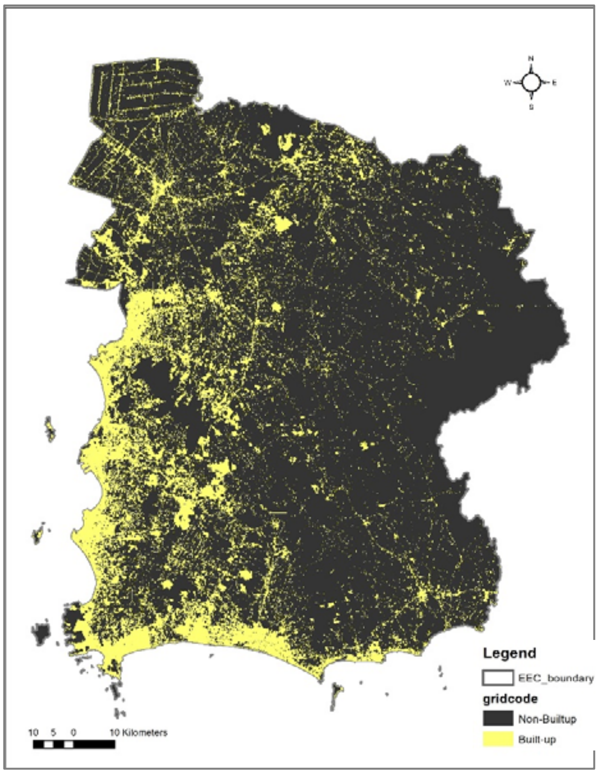

Land use 2016

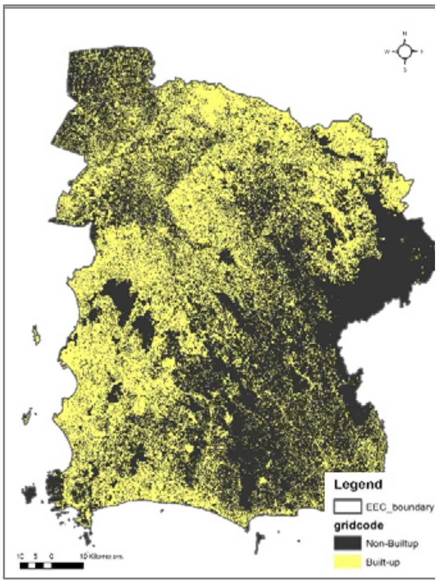

NDBI

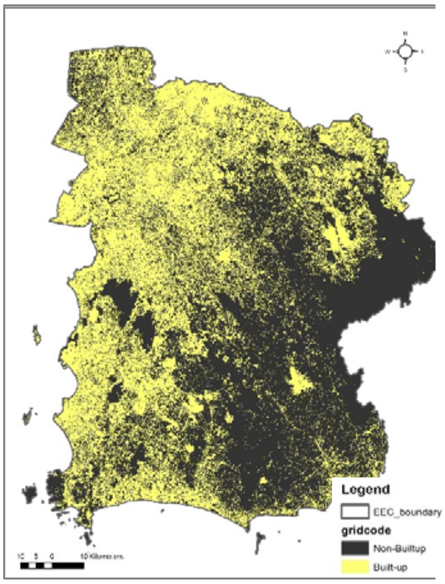

BUI

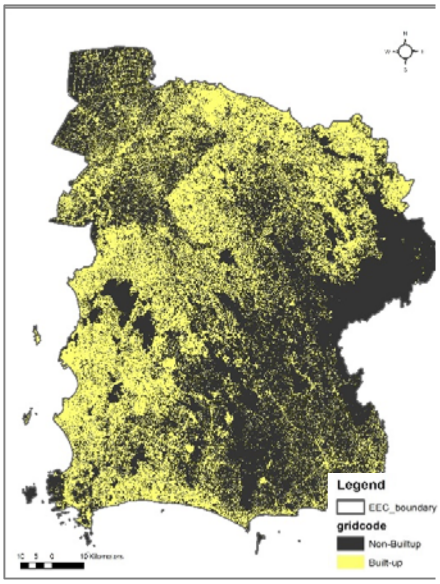

MBUI

(1) Otsu’s thresholding method

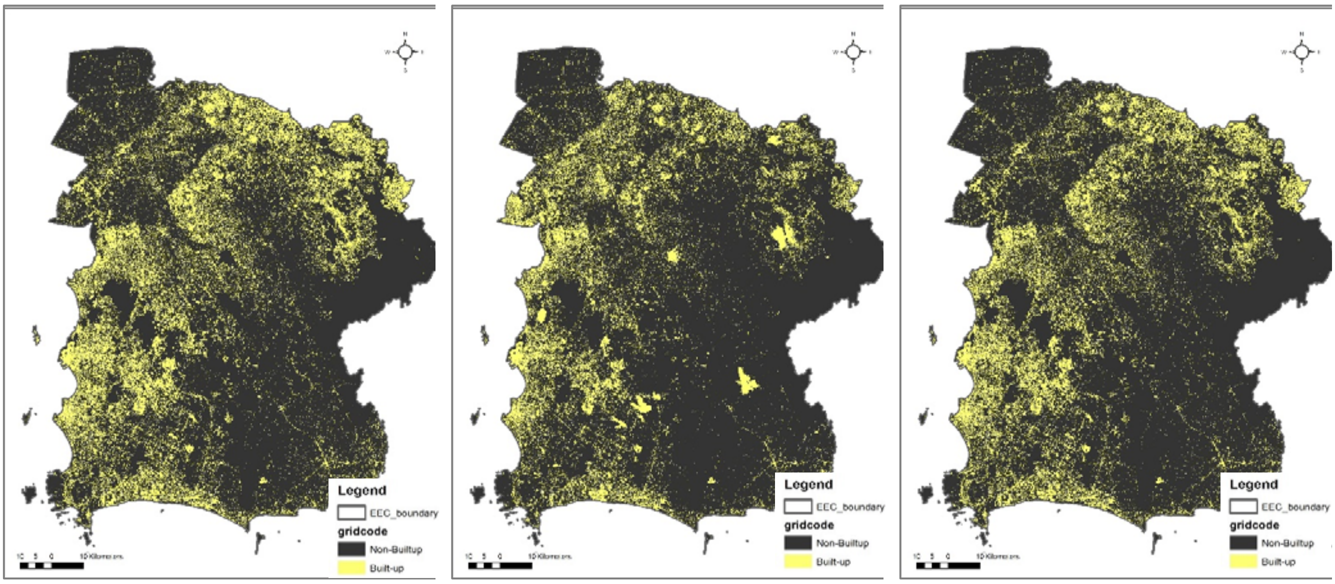

NDBI BUI MBUI

(2) Otsu's thresholding method in AoL

Fig. 6 Built-up areas from land-use 2016, and (1) the satellite image extraction results using indices and Otsu's thresholding method, and indices, (2) Otsu's thresholding method with the integration of Ao

ACKNOWLEDGMENT

We would like to thank the Geoinformatics and Space Development Agency (GISTDA), Thailand for sources of geographical data. Additionally, we also highly appreciate the help from Nuntikorn Kitratporn, who dedicated her time to proofread the manuscript.

REFERENCES

[1] T. Ferreira, "Using satellite data to track socio-economic outcomes: a case study of Namibia," *Work. Pap.*, 2018.

[2] W. Prasomsup, P. Piyatadsananon, W. Aunphoklang, and A. Boonrang, "Extraction technic for built-up area classification in Landsat 8 imagery," *Int. J. Environ. Sci. Dev.*, vol. 11, no. 1, pp. 15–20, 2020, doi: 10.18178/ijesd.2020.11.1.1219.

[3] I. N. Hidayati and R. Suharyadi, "A Comparative Study of various Indices for extraction urban impervious surface of Landsat 8 OLI," *Forum Geogr.*, vol. 33, no. 2, pp. 162–172, 2019, doi: 10.23917/forgeo.v33i2.9179.

[4] V. S. Bramhe, S. K. Ghosh, and P. K. Garg, "Extraction of Built-Up Area by Combining Textural Features and Spectral Indices from Landsat-8 Multispectral Image," *ISPRS - Int. Arch. Photogramm. Remote Sens. Spat. Inf. Sci.*, vol. XLII–5, no. November, pp. 727–733, 2018, doi: 10.5194/isprs-archives-xlii-5-727-2018.

[5] M. K. Firozjaei, A. Sedighi, M. Kiavarz, S. Qureshi, D. Haase, and S. K. Alavipanah, "Automated built-up extraction index: A new technique for mapping surface built-up areas using LANDSAT 8 OLI imagery," *Remote Sens.*, vol. 11, no. 17, 2019, doi: 10.3390/rs11171966.

[6] A. Rasul *et al.*, "Applying built-up and bare-soil indices from Landsat 8 to cities in dry climates," *Land*, vol. 7, no. 3, 2018, doi: 10.3390/land7030081.

[7] S. S. Bhatti and N. K. Tripathi, "Built-up area extraction using Landsat 8 OLI imagery," *GIScience Remote Sens.*, vol. 51, no. 4, pp. 445–467, 2014, doi: 10.1080/15481603.2014.939539.

[8] R. Goldblatt *et al.*, "Using Landsat and nighttime lights for supervised pixel-based image classification of urban land cover," *Remote Sens. Environ.*, vol. 205, no. February 2017, pp. 253–275, 2018, doi: 10.1016/j.rse.2017.11.026.

[9] J. C. Duque, N. Lozano-Gracia, J. E. Patino, P. Restrepo, and W. A. Velasquez, "Spatiotemporal dynamics of urban growth in Latin American cities: An analysis using nighttime light imagery," *Landsc. Urban Plan.*, vol. 191, no. January, 2019, doi: 10.1016/j.landurbplan.2019.103640.

[10] X. Liu *et al.*, "High-resolution multi-temporal mapping of global urban land using Landsat images based on the Google Earth Engine Platform," *Remote Sens. Environ.*, vol. 209, no. January, pp. 227–239, 2018, doi: 10.1016/j.rse.2018.02.055.

[11] D. C. Pu, J. Y. Sun, Q. Ding, Q. Zheng, T. T. Li, and X. F. Niu, "Mapping Urban Areas Using Dense Time Series of Landsat Images and Google Earth Engine," *Int. Arch. Photogramm. Remote Sens. Spat. Inf. Sci. - ISPRS Arch.*, vol. 42, no. 3/W10, pp. 403–409, 2020, doi: 10.5194/isprs-archives-XLII-3-W10-403-2020.

[12] R. Goldblatt, W. You, G. Hanson, and A. K. Khandelwal, "Detecting the boundaries of urban areas in India: A dataset for pixel-based image classification in google earth engine," *Remote Sens.*, vol. 8, no. 8, 2016, doi: 10.3390/rs8080634.

[13] P. Guruprasad, "Overview of Different Thresholding Methods in Image Processing," *TEQIP Spons. 3rd Natl. Conf. ETACC*, no. June, 2020.